Clinical and Translational Radiation Oncology 3 (2017) 1–8

Contents lists available at ScienceDirect

Clinical and Translational Radiation Oncology

journal homepage: www.elsevier.com/locate/ctro

Review Article

The clinical target volume in lung, head-and-neck, and esophageal cancer: Lessons from pathological measurement and recurrence analysis

Rudi Apolle [a,b,*], Maximilian Rehm [b,c,d], Thomas Bortfeld [e], Michael Baumann [a,b,c,d,f,g], Esther G.C. Troost [a,b,c,d,f]

[a] Helmholtz-Zentrum Dresden-Rossendorf, Institute of Radiooncology – OncoRay, Dresden, Germany
[b] OncoRay – National Center for Radiation Research in Oncology, Dresden, Germany
[c] Department of Radiation Oncology, University Hospital and Medical Faculty Carl Gustav Carus, Technische Universität Dresden, Dresden, Germany
[d] German Cancer Consortium (DKTK), Partner Site Dresden, Dresden, Germany
[e] Department of Radiation Oncology, Massachusetts General Hospital and Harvard Medical School, Boston, MA, USA
[f] National Center for Tumor Diseases (NCT), Partner Site Dresden, Dresden, Germany
[g] German Cancer Research Center (DKFZ), Heidelberg, Germany

ARTICLE INFO

Article history:
Received 5 December 2016
Revised 19 January 2017
Accepted 19 January 2017
Available online 21 March 2017

Keywords:
Microscopic tumor extension
Clinical target volume
Adaptive radiotherapy
Particle beam irradiation

ABSTRACT

Radiotherapy research has achieved remarkable progress in target volume definition. Advances in medical imaging facilitate more precise localization of the gross tumor volume, alongside a more detailed understanding of the geometric uncertainties associated with treatment delivery that has enabled robust safety margins to be customized to the specific treatment scenario at hand. By contrast, the clinical target volume, meant to encompass gross tumor, as well as, adjacent sub-clinical disease, has evolved very little. It is more often defined by clinician experience and institutional convention than on a patient-specific basis. This disparity arises from the inherent invisibility of sub-clinical disease in current medical imaging. Its incidence and expanse can only be ascertained via indirect means. This article reviews two such strategies: histopathological measurements on resection specimen and analyses of locoregional recurrences after radiotherapy.

Contents

* Corresponding author at: Helmholtz-Zentrum Dresden-Rossendorf, Institute of Radiooncology, Bautzener Landstrasse 400, 01328 Dresden, Germany. Fax: +49 (0) 351 458 5716.
E-mail address: apolle@hzdr.de (R. Apolle).

http://dx.doi.org/10.1016/j.ctro.2017.01.006
2405-6308/

Introduction

Precise tumor localization is of utmost importance in the new era of high-precision radiotherapy (RT) delivered using photons or particles, and possibly even more so when adapting treatment during the course of irradiation. The creation of the target volume to be irradiated is a multi-step process. First, the radiation oncologist delineates the gross tumor volume (GTV; primary tumor and metastatic lymph nodes) visible on imaging (computed tomography, CT; magnetic resonance imaging, MRI; positron emission tomography, PET). It is known that most solid tumors exhibit microscopic tumor extension (ME) not manifest in clinical imaging. Thus the GTV is expanded by an empirically defined margin to the so-called clinical target volume (CTV), encompassing both macro- and microscopic tumor. Most treatment schedules are delivered throughout the course of several weeks. Therefore, another margin is added compensating for random and systematic setup errors occurring during treatment delivery, leading to the planning target volume that is to be irradiated (PTV).

In past years, RT-based research has focused on exact demarcation of the GTV with modern imaging techniques and on measurement-driven PTV definitions precisely compensating the setup uncertainties encountered [*e.g.* 1,2]. With these advances GTV and PTV can be tailored to individual patients. Incongruously, the CTV is still defined using non-individualized population-based empirical margins for all tumors of a given type in a given anatomical location. Moreover these margins are based on a few, mostly outdated studies, not utilizing modern pathological analysis techniques and unable to align and correlate findings with current medical imaging. This lack of knowledge may lead to excessive toxicity via overly generous margins, or to underestimation of the true extent of disease and likely recurrence. Modern RT delivery options stand to add another layer of complexity to this matter. Particle therapy, characterized by its steep dose fall-off distal to the Bragg peak, will offer less tolerance to underestimation of the target extent, while adaptive highly conformal strategies will need to consider the possibility of sub-clinical and gross disease evolving differently.

This review focuses on solid tumor types in which (adaptive) radio(chemo)therapy (using photons or particles) frequently is the only or the neoadjuvant treatment modality, and in which retrospective data on CTV have been published and can also be prospectively gathered. It covers series assessing the ME on a histopathological basis and publications on recurrence patterns. These two fields of study attempt to refine the CTV from opposing yet complementary viewpoints. The former directly probes the underlying pathology necessitating a CTV and is the best source of information for its design. The latter, more inclusive, approach can test the adequacy of CTV definition in clinical practice and also serves to evaluate its importance relative to other current concerns. The review concludes with a discussion including recommendations for future research.

Pathological measurement of microscopic tumor extension

This section describes the available literature covering measurements of ME in various solid tumors. Given its inherent invisibility in clinical imaging, ME can only be directly assessed in resection specimen. Aided by pathologists, researchers from the disciplines of surgery and radiooncology have hence performed investigations of this type in order to determine margin widths around the GTV, which encapsulate ME in a certain percentage of patients.

The general procedure of these investigations is fairly universal. Resection specimen undergo the standard histological processing yielding stained microscopic slides. Gross tumor is delineated either on these slides or on co-registered photographs of macroscopic thick slices taken after fixation. In either case delineation is usually performed without magnification. Conversely, ME is delineated under the microscope and identified as small tumor islets.

In order to be useful for RT planning, measurements on resection specimen must be translated to the *in-situ* tissue geometry. Depending on the tumor site this can represent an immense challenge, since deformations occur both upon removal of the tissue, as well as during the subsequent histological processing. A particular focus of this section will thus be to examine the way in which various groups have tried to ensure a geometric correspondence between the two states.

The following subsections discuss ME measurements around primary tumors originating in the lung, head-and-neck region, or esophagus. A summary of the spatial information contained in the reviewed literature is provided in Fig. 1. An overview of ME of nodal targets as well as other tumor entities can be found in a comprehensive review by Moghaddasi et al. [3].

Non-small cell lung cancer

There is a comparative wealth of histopathological studies concerned with non-small cell lung cancer (NSCLC) and its ME. Concentrating on the most modern research, a total of six analyses were available for this review. Most of them focus on the distribution of maximal ME, *i.e.*, the distance from the gross tumor edge to the farthest instance of ME detected in the whole specimen. Many studies investigate the influence of some property of the lesion on the extent of ME. Two of those were considered in more than one publication, namely the histological type and grade.

Kara et al. [4] analyzed 70 specimen obtained through various lung resection techniques. Their focus lay in examining tumor infiltration along the bronchial wall, in particular in the proximal direction. Fresh specimen were sectioned at predetermined distances from the gross tumor to yield transverse slices of the bronchus concerned. This allowed for quantification of the ME distance unencumbered by deformations suffered as a consequence of histological processing, albeit at a rather coarse resolution of 5 mm in most cases. Thirty-four specimen exhibited ME, with half of the observed instances directly abutting the gross tumor. Squamous cell carcinoma (SCC) had a higher likelihood than adenocarcinoma (ADC) of any ME being present, while in specimen positive for ME its extent was higher in ADC than SCC. The 86th and 93rd percentile of the inclusive ME distribution were located at 10 mm and 15 mm, respectively.

Giraud et al. [5] studied ME in 42 pneumonectomy and lobectomy specimen representing various stages of ADC and SCC. Tissue deformation was controlled by first gently inflating the specimen with the fixation agent and then selecting only those slides for analysis, which appeared well-insufflated (*i.e.* not exhibiting collapse of alveolar structures). The analysis revealed a significant difference in the extension distances for SCC and ADC, the respective mean measurements being 1.5 ± 2.4 mm and 2.7 ± 2.8 mm. The authors further report that the necessary margins required to encompass 95% of ME are 6 mm and 8 mm, respectively. These figures should be interpreted with caution, however, since this is one of the few studies reporting the ME measurements for each individual slide, not just the maximum value per patient. The quoted widths therefore apply to margins suitable to capture ME in a fraction of all histological slides. Without knowledge of how these slides are distributed among patients one cannot necessarily conclude that the suggested margins would cover all ME for said percentage of patients.

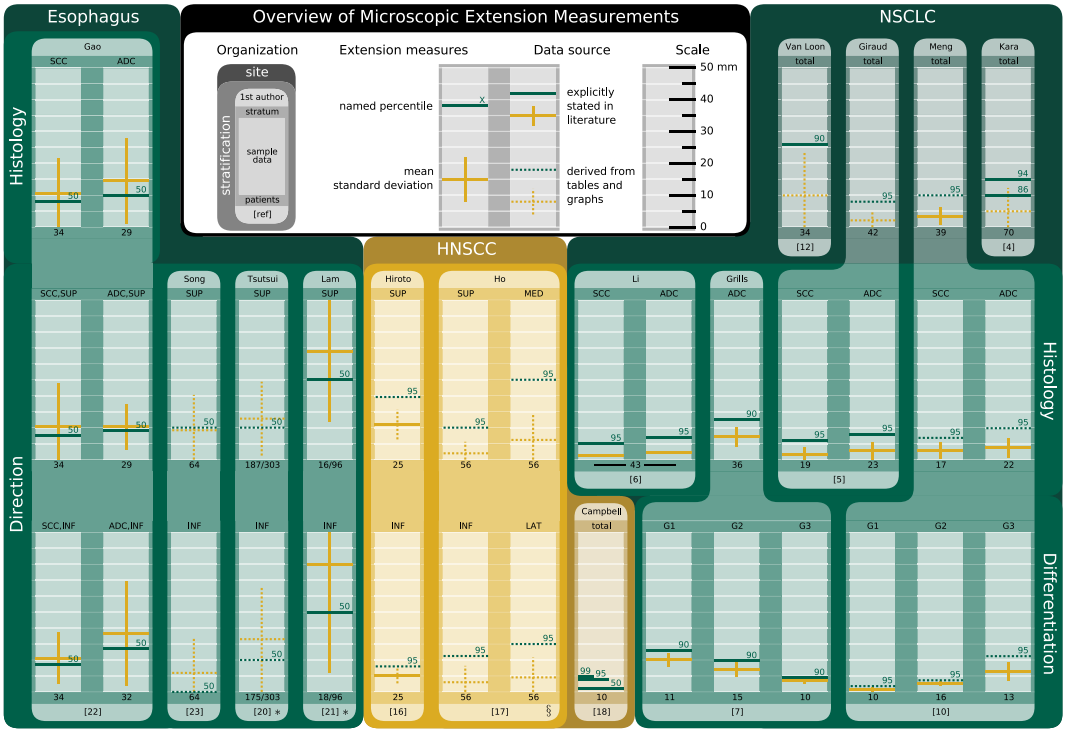

Fig. 1. Graphical overview of microscopic extension summary statistics meant to encourage a broad assessment of compatibility between the various studies. Values for each sample are marked as colored lines (yellow: mean and standard deviation; green: named percentile) on a 50 mm scale with 5 mm sub-divisions. Green numbers above lines indicate the percentile whose value is reported. Values were taken directly from the source texts if available (solid lines). Otherwise values were estimated from tables and graphs (dotted lines). If extension data was grouped into bins, their upper edges were used for calculation in the latter case, *e.g.* if five instances of infiltration were observed at distances of 10–15 mm, an extension distance of 15 mm was assigned to all five cases. Tumor sites are demarcated by colored panels and labeled at the top of each panel. More lightly tinted panels of the same primary color indicate stratification by attributes listed on the sides, while the stratum each sample belongs to is given directly above its scale. Darker shades of the primary color signify results for un-stratified samples. Individual studies are identified by tabs on the upper (first author) and lower (reference number) edge of a lighter shape surrounding the scales and linking them across different stratifications. Measurements are generally reported for the entire cohort (*i.e.* including extension-negative samples) and the sample size is given underneath each scale. Abbreviations: ADC, adenocarcinoma; SCC, squamous cell carcinoma; NSCLC, non-small cell lung cancer; HNSCC, head-and-neck SCC; SUP, superior; INF, inferior; MED, medial; LAT, lateral; G, histological grade. *Notes*: *Results are plotted for extension positive samples only and the positive ratio is given underneath; §Excludes measurements from one outlying patient. (For interpretation of the references to color in this figure legend, the reader is referred to the web version of this article.)

Li et al. [6] reported on the analysis of ME in 43 resection specimen. Despite its full-text only being available in Chinese, this investigation has received many citations in the English literature. The abstract lists significantly different mean values of ME distance for ADC (2.2 mm) and SCC (1.3 mm), confirming the observation made by Giraud et al. [5]. The authors recommend respective margins of 7 mm and 5 mm to cover ME in 95% of cases.

Grills et al. [7] performed a study of 35 pT1N0M0 ADC specimen obtained either by wedge resection or by completion lobectomy. No deformation correction was performed, with the authors arguing that the peripheral lesion sites meant that there was little lung parenchyma, which could have been re-expanded, and, moreover, little deformations due to fixation were expected as a result of the sparsity of myofibroblastic cells and smooth muscle in the specimen. The average maximal extension distance measured for the whole sample was 7.2 ± 3.1 mm. Special attention was paid to recording the amount of tissue along the tumor radius exhibiting a so-called lepidic growth pattern. This histomorphological trait entails infiltration purely along pre-existing alveolar structures, devoid of desmoplasia and causing very little inflammation [8]. It is characteristic of a range of ADC precursor lesions, which until 2011 were subsumed under the term bronchiolo-alveolar carcinoma (BAC), but have since been re-classified into five different entities [9]. Grills et al. [7] found a relationship of the percentage of BAC involvement with ME, greater involvement being associated with farther extension. Quantitatively this relationship is reported in terms of histologic grade. More highly differentiated specimen showed significantly higher percentages of BAC involvement and hence also larger mean maximal extension distances. The measurements for grades 1, 2, and 3 were 10.1 ± 2.1 mm, 7.0 ± 2.2 mm, and 3.5 ± 0.8 mm, respectively.

Meng et al. [10] examined specimen from 39 patients with the ultimate aim of finding correlations between the ME distance and quantitative [^{18}F]fluorodeoxyglucose (FDG)-PET imaging features. All but one specimen exhibited ME, and the overall mean maximal extension distance was 3.4 ± 2.8 mm. They analyzed both ADC and SCC, but found no significant difference in the spread of ME between the two samples, their respective mean maximal ME measurements being 3.8 ± 3.0 mm and 2.9 ± 2.6 mm. No attempt was made to correct for tissue deformations, while the authors do acknowledge that they observed shrinkage due to fixation by around 18% in a similar study [11]. A significant difference was revealed when the influence of histologic grade was examined, with more highly differentiated tumors showing smaller maximum extension distances on average for either histological type. The corresponding measurements were 0.9 ± 0.7 mm, 2.6 ± 0.7 mm, and 6.3 ± 2.9 mm, for grades 1, 2, and 3, respectively, including both histologic types. This stands in stark contrast to the findings of Grills et al. [7] who reported an inverse relationship for their sample of peripheral low-stage ADC. Finally the authors discuss the predictive power of two FDG-PET features, namely maximum standardized uptake value (SUVmax) and metabolic tumor volume (delineated using an SUV threshold of 2.5), which were

both shown to be positively and significantly correlated with ME distance.

Van Loon et al. [12] reported an analysis of 34 lobectomy specimen of varying histologic type and location, ultimately trying to develop a prediction model for the presence of ME based on quantitative imaging parameters. The investigation utilizes a careful procedure for re-establishing the *in vivo* configuration of the specimen developed by Stroom et al. [13] and combines it with a two-step registration sequence to establish correspondence between pre-treatment imaging and macroscopic photographs of the sliced specimen. This procedure was reported upon separately by Siedschlag et al. [14] who also quantified the magnitude of lung tissue deformations. The somewhat disturbing conclusion was that uncorrected measurements of this type might underestimate the true extent of ME by a factor of 1.6. Van Loon et al. [12] observed ME in half of the specimen studied, distributed such that a margin of 26 mm would be required to cover ME in 90% of the entire cohort (including ME negative specimen). As for the prediction model, they identified two parameters, which were significantly associated with the presence of ME in a multivariate logistic regression: the GTV on CT and the mean Hounsfield unit measured across the GTV.

The above studies agree encouragingly well in some regards, especially as far as the influence of histologic type is concerned, while no clear picture emerges as to the effect of histologic grade. Worryingly, the study employing the most elaborate geometric corrections reports the largest extension distances.

Head-and-neck cancer

While there are a fair number of studies concerned with mapping the likelihood of regional lymphatic infiltration, literature on the subclinical extent of primary head-and-neck squamous cell carcinoma (HNSCC) is relatively sparse. This site tends to suffer less from tissue deformations due to the rigidity of the cartilage structures. A very detailed procedure for controlling and correcting such deformations has been presented by Caldas-Magalhaes et al. [15], but so far not used to quantify ME.

Hiroto et al. [16] analyzed 29 pharyngolaryngoesophagectomy specimen. The collective longitudinal spread of all lesions ranged from the epiglottis to the sixth tracheal cartilage, while tumor was present at the height of the cricoid in all specimen. Circumferential involvement of the mucosal layer, as well as infiltration into the innermost muscle layer was observed in more than 70% of cases. At farther radii longitudinal spread was the dominant extension pattern, possibly along the various lymphatic networks in the mucosal layers. In the 25 cases exhibiting this pattern, proximal extension was more expansive than distal spread, with respective mean infiltration distances of 11 mm and 5 mm.

Ho et al. [17] measured the incidence and extent of submucosal tumor spread in 57 hypopharyngeal SCC specimen. In order to limit tissue deformations, fresh specimen were pinned onto boards prior to fixation. ME was identified under a microscope and its distance measured both laterally and longitudinally from the ulcer edge. While the lateral measurements were performed directly on the slide, the longitudinal distance was inferred from the number of slides separating the tumor edge from the ME and thus limited in resolution by the section thickness of 3–5 mm. ME was identified in 33 specimen (58%) with directional incidences of 16% and 28% for the superior and inferior directions, and 37% and 26% for the medial and lateral directions, respectively. Excluding measurements for one outlying specimen which showed extended lymphatic spread, the maximal extents in each direction were 10 mm (superior), 20 mm (inferior), 25 mm (medial), and 20 mm (lateral).

Campbell et al. [18] performed a study of 10 pT1-T3 SCC specimen of the tongue. Tissue deformations were measured and corrected by encasing the specimen in agarose prior to fixation. Since shrinkage due to fixation is mostly confined to the specimen itself, the resulting deviation of the specimen contour from that of the agarose can be used to derive a suitable deformable registration to establish correspondence between the two geometries. ME was observed in half of the analyzed histologic slides, with most instances directly abutting the GTV and only around a quarter being separated from it. The 50th, 95th, and 99th percentiles of the distribution of extension distances were 1.0 mm, 4.0 mm, and 4.8 mm, respectively.

While limited in number, the above results hint at quite different distributions of ME for different sites within the field of HNSCC.

Esophageal cancer

Numerous studies have assessed ME of esophageal tumors, mostly in order to define safe longitudinal resection margins. The four publications reviewed below provide more detail of the spatial distribution of ME around the primary tumor, with two specifically setting out to determine adequate CTV margins. Three of these studies solely assessed SCC, whereas the fourth analysis also included ADC of the gastro-esophageal junction. Esophageal specimen exhibit pronounced shrinkage from their *in-situ* size. In an analysis of 55 specimen Siu et al. [19] found a shortening of the distal and proximal resection margins to around a third, while tumors retained 90% of their original length. Attempts at mitigation range from stretching the specimen to its *in-situ* length and pinning it to a board to simply correcting measurements by a shrinkage factor determined for the specimen as a whole.

Tsutsui et al. [20] reported on the analysis of 303 patients with pT1-4 SCC located in all three sections of the esophagus. The authors observed ME proximal and distal to the tumor in 187 and 175 cases, respectively, and found 94% and 83% of those lesions to lie within 30 mm of the tumor edge. Concerning intra-epithelial ME, the investigators differentiated between contiguous and isolated cases and found their maximal extent to be 30 mm and 120 mm, respectively. The maximal distance for subepithelial extension was 106 mm, and that for spread along lymphatic or vascular pathways 79 mm. Noteworthily, this is the only study permitting neoadjuvant radio(chemo)therapy. In most neoadjuvantly treated patients, however, a complete tumor response or reepithelization was found such that an adequate evaluation of the ME was not possible.

Lam et al. [21] analyzed 96 patients with pT1-4 SCC destroying the basement membrane or primarily growing subepithelially with known accessory lesions. They identified ME in 25 specimen and measured extension distances of 34 ± 22 mm (range: 5–77 mm) proximally and 40 ± 34 mm (range: 5–95 mm) distally for this group.

Gao et al. [22] published the first prospective study explicitly seeking to define CTV margins. Sixty-six patients with pT1-4 esophageal SCC or ADC of the gastro-esophageal junction were included. SCC showed respective mean ME distances of 10.5 ± 13.5 mm and 10.6 ± 8.1 mm, for the proximal and distal directions, with 94.1% and 97% of all lesions located within the first 30 mm. For ADC these measurements are stated as 10.3 ± 7.2 mm proximally and 18.3 ± 16.3 mm distally. Remarkably, all instances of proximal ME were found within 3 cm of the primary tumor while a 5 cm margin around it would only have covered 93.8% of distal extensions. The authors conclude that the CTV margin should be 3 cm in both directions for SCC, and 3 cm proximally and 5 cm distally for ADC.

Song et al. [23] analyzed 64 pT2-3 SCC specimen. Subepithelial, intraepithelial and dysplastic lesions were considered ME and their

incidence recorded in successive 1 cm bands around the main lesion. A significant reduction of incidence with increasing distance was revealed. Within the first centimeter, 53.1% (proximal) and 32.8% (distal) of all cases exhibited ME, while only 3.6% (either direction) did so at distances of 3–4 cm. The authors conclude by recommending CTV margins extending 3 cm proximally and 4 cm distally from the GTV to cover 95% of all lesions.

The limited number of high-quality publications have thus far only investigated the effect of histological subtype and location. No correlations with other tumor characteristics have been published.

Recurrence analysis after definite radio(chemo)therapy

Tumor recurrence is affected by the entire spectrum of treatment decisions, such that its investigation offers the most thorough and realistic test of geometric and dosimetric treatment adequacy. This also makes it difficult to assess the influence of any particular aspect in isolation. As far as the CTV is concerned the most that can usually be ascertained is if the CTV definition within a particular treatment regimen is sufficient or not, unless studies were specifically designed to be sensitive to this aspect. One must also be very cautious when drawing general conclusions from these results, since they cannot easily be transferred to other treatment strategies (*e.g.* irradiation technique, chemotherapy).

Most of the reviewed studies retrospectively analyze the imaging data acquired at the time when recurrence was identified and try to relate its location back to the original planning volumes or dose distribution. In order to do so, some form of deformable image registration has to be applied. Recurrences can then be classified as in-field (IF), marginal (MA), or out-of-field (OF) with reference to either the target volumes or dose distribution. Two varieties of the geometric approach are employed in the literature. Classification is either based on the fraction of the recurrence volume overlapping with the target volumes, or the distance between the likely point of origin (nidus, center of mass) of the recurrence and the target volume boundary. The former approach has a tendency to assign recurrences to more peripheral locations as they grow,

Table 1
Summary of recurrence analyses after definite radio(chemo)therapy for head-and-neck squamous cell carcinoma and lung cancer.

Reference	Site	Target volume construction		Dose [Gy] / Technique	Cohort / Follow-up*	Recurrences: Methodology	Type	IF	MA	OF
Dandekar *et al.* [28]	HNSCC	CTV-HD	(GTVp + 5-10 mm) + GTVn	70	114 total	dosimetric	local	12	0	0
		CTV-ID	some LNL	59	18 recurred		regional	10	0	
		CTV-LD	some uninvolved LNL	54	median 29* months					
		PTV	CTV + 3-5 mm	IMRT (HT)						
Due *et al.* [29]	HNSCC	CTV-HD	GTV + 10 mm	66 or 68	520 total	center of mass		47	0	1
		CTV-ID	CTV-HD + 2 mm + HR LNL	60	304 responsive					
		CTV-LD	CTV-ID + 2 mm + LR LNL	50	100 recurred					
				IMRT	39 analyzed					
					median 17 months					
Bayman *et al.* [31]	HNSCC non-naso-pharyngeal	CTV-HD	(GTVp + 10 mm + compartment) + involved LNL	70	136 total	dosimetric	local	4	1	1
					120 responsive		regional	1	0	
		CTV-ID	some uninvolved LNL	63	7 recurred					
		CTV-LD	some uninvolved LNL	57	median 31 months					
		PTV	CTV + 4 mm	IMRT						
Ferreira *et al.* [33]	HNSCC	CTV-HD	GTVp + large adenopathies	59-70	367 total	target volume	local	1	12	8
		CTV-ID	EORTC consensus guidelines	50-59	22 recurred		regional	1	6	
				3D-CRT	mean 17 months	center of mass	local	11	1	9†
				IMRT			regional	3	4	
						dosimetric	local	10	3	8
							regional	2	5	
De Felice *et al.* [34]	HNSCC	CTV-HD	(GTVp + 10 mm + compartment) + (GTVn + 10 mm)	65	653 total	dosimetric	local	33	0	2
					56 analyzed		regional	32	0	1
		CTV-LD	EORTC consensus guidelines	54	median 14 months					
		PTV	CTV + 4 mm	IMRT						
Liang *et al.* [25]	NSCLC	two arms:	CTV = GTV + 6 or 8 mm	54-63	50 total, 16 rec.	location relative to PTV margin	local	15	1	0
			CTV = GTV without expansion		55 total, 18 rec.		local	17	1	0
		PTV	ITV(3-15 mm) + 5 mm	IMRT						
Kilburn *et al.* [27]	NSCLC SCLC	CTV	GTV without expansion	45-74	110 total	location relative to PTV margin	local	12	0	2
		PTV	ITV + 5 mm	3D-CRT	20 recurred		regional	2	2	4
				IMRT						

Abbreviations: HNSCC, head-and-neck squamous cell carcinoma; (N)SCLC, (non-)small cell lung cancer; GTV(p/n), (primary/nodal) Gross Tumor Volume; (C/I/P)TV, (Clinical/Internal/Planning) Target Volume; (H/I/L)D, (high/intermediate/low)-dose; (H/L)R, (high/low)-risk; LN(L), lymph node (level); RT, radiotherapy; 3D-CRT, three-dimensional conformal RT; IMRT, intensity-modulated RT; HT, helical tomotherapy; IF, in-field; MA, marginal; OF, out-of-field.
Notes: *Follow-up times are stated for the entire cohort, apart from the marked instance, where the period for survivors is quoted instead; †Eight recurrences were consistently classified as OF, while the center of mass method assigned an additional local recurrence to this category.

while the latter assumes an isotropic growth of the recurrence, which is unrealistic in some scenarios [24]. Classification by the dosimetric route is based on the overlap of the recurrence volume with some planned isodose (typically at 95% of the prescribed dose).

This section covers recurrence analyses on NSCLC and HNSCC only, since the preferred treatment modality for esophageal cancer is neoadjuvant radiochemotherapy followed by surgery, such that their respective influences cannot be disentangled. A summary of study parameters and results is provided in Table 1.

Non-small cell lung cancer

Liang et al. [25] studied 105 patients with stage III NSCLC, who underwent radio(chemo)therapy either with (50) or without (55) a CTV margin as suggested by Giraud et al. [5]. Roughly a third of either group suffered local relapse, which was mostly confined within the PTV. MA recurrences were observed for one patient in each group. Most comparisons of treatment outcome in the two groups did not reveal any significant differences, the only exception being the incidence and grade of radiation-induced pneumonitis, which was higher in the with-CTV arm. An earlier study [26] had already revealed similarly low rates of MA recurrence in small cell lung cancer. Ultimately the authors suggest foregoing the CTV altogether either to allow for isotoxic dose escalation, or to reduce the incidence of pneumonitis.

Kilburn et al. [27] reviewed 110 cases of various cancers of the lung treated with either three-dimensional conformal RT (3D-CRT) or intensity-modulated RT (IMRT). Common to both irradiation techniques was the omission of a CTV during planning. The 4D-PET/CT-based GTVs were first transformed into an internal target volume (ITV) and then expanded by 5 mm to form the PTV. Twenty-two recurrence volumes were identified in 20 patients. Recurrences were classified by their location (whose exact determination is not specified) to either have occurred inside the PTV (IF), away from it (OF), or within a 10 mm margin around it (MA). This latter assignment represents recurrences, which might have been encompassed by a CTV margin of 10 mm. Only two such recurrences were identified, both adjacent to a nodal target, while the predominant mode of failure was IF. The relative lack of MA recurrences is attributed to the use of FDG-PET in the majority of cases and daily cone beam imaging for setup verification. The authors conclude by arguing that the omission of larger margins seems feasible and abandoning the CTV as a whole might be justified in order to improve the therapeutic ratio.

Head-and-neck cancer

The treatments analyzed by the following studies employed a two- or three-tiered dose painting strategy. CTV delineation practices differed in the method of expanding the GTV (volumetric or anatomic) and the assignment of lymphatic regions to high-, intermediate- or low-dose target volumes (Table 1). A particular interest of many studies is to determine whether the advent of IMRT with dose gradients steeper than those achieved with 3D-CRT has caused an increase in MA failures, which would indicate that clinical margins are too narrow.

Dandekar et al. [28] studied recurrences in 114 HNSCC patients treated with helical tomotherapy. Twenty-two recurrences were observed in 18 patients, twelve of them local and ten regional. All were classified as IF using the requirement that at least half of the recurrence volume was contained within the planned 95% isodose. In light of these and similar findings, the authors suggest that "only a minimal (if any) CTV margin is required beyond a carefully contoured GTV".

Due et al. [29] analyzed recurrences after 520 IMRT treatments of HNSCC. Out of the 304 patients who initially achieved complete response, 69 suffered loco-regional recurrences. Thirty-nine cases comprising 48 recurrence volumes were available for analysis. Using a center of mass method all but one recurrence were identified as IF, the other OF. Additionally the investigators calculated the spatial density of recurrences for the entire cohort and different volumes. Using FDG-PET-based regions of interest, constructed as iso-SUV contours relative to SUVmax, they found that the chosen SUV percentage was significantly and positively correlated with recurrence density, suggesting that such a feature could be used for dose-redistribution [30].

Bayman et al. [31] analyzed treatment outcomes in a cohort of 136 patients who underwent IMRT for various non-nasopharyngeal HNSCC. Among the 120 patients who initially experienced complete response, seven recurrences were diagnosed and - based on the fraction of the recurrence volume (deformably registered to the planning CT) covered by the 95% isodose - classified as IF (5), MA (1), and OF (1). The authors compared their results to an earlier study performed at their institute with 3D-CRT, which gave comparable rates of MA and OF recurrences [32], and conclude that IMRT has not lead to significant undertreatment in the margins and IF recurrences remain the major cause of failure.

Ferreira et al. [33] investigated recurrences in various HNSCC. The investigation utilized data from 367 patients, treated both definitely and adjuvantly, and with both 3D-CRT and various types of IMRT, including adaptive therapy in 22 patients. A special focus of the analysis was to determine the level of agreement between the three common methods of classifying recurrences. Overall the authors observed 13 local, 7 regional and 8 distant recurrences, the latter of which were rated OF by all three classification methods. There was a disparity between the classifications of IF and MA recurrences, with the center of mass and dosimetric methods largely agreeing. The method based on the overlap between the recurrence volume and the CTV had a tendency to identify recurrences as MA, the trend being more marked for local recurrences. The 13 recurrences of this type were classified as 11 IF, 1 MA, and 1 OF by the center of mass method. While this is broadly compatible with the dosimetric assignment of 10 IF and 3 MA, it differs extensively from the classification relative to the CTV, which yielded 1 IF and 12 MA.

De Felice et al. [34] reviewed a large cohort of 653 HNSCC treated with RT. Among the patients who underwent primary IMRT, 56 suffered recurrences, which were predominantly classified as IF by a dosimetric method. Out of 68 recurrence volumes (35 local, 33 regional) none were classified MA and three as OF (2 local, 1 regional). The treatments reviewed used both a volumetric, as well as an anatomic expansion to derive the primary CTV. Given the results, the authors tentatively argue that the high percentage of IF recurrences indicate that anatomic expansion could be foregone provided a sufficient volumetric margin (10 mm) is used to define the CTV.

Discussion and outlook

This review summarizes relevant and well-documented findings on microscopic tumor extension measured in resection specimen and recurrence patterns after RT with variously defined CTVs, including deliberate omission of the CTV margin.

Regarding the first, some important limitations became apparent, with geometric concerns most widely acknowledged. The confidence with which ME measurements can be translated into CTV margin recommendations is limited by tissue deformations, as well as the incongruence of the GTV *in vivo* and in imaging.

A second limitation arises from the nature of the specimen available for study. Since they are mostly obtained through primary resection, they might not be representative of the spectrum of disease primarily treated with RT. This also precludes assessments of the influence of neoadjuvant radio(chemo)therapy on the distribution of ME, which are vital for CTV design in the adaptive setting. Tumors, for which a tri-modality approach is state-of-the-art, *e.g.*, esophagus or rectum, are the most appealing candidates for study in this regard.

An issue rarely commented upon is sensitivity. Sparse sampling of the specimen and a lack of sensitivity to single cell migration both restrict the efficiency with which ME can be detected. These investigations are a very laborious endeavor and complete histologic sampling is unfeasible, but an estimate of the detection efficiency should be obtained and propagated to the results. Histologic tumor markers might improve the sensitivity to smaller clusters of infiltrating cells.

Lastly, only the influence of rather basic tumor characteristics on ME has been analyzed. With the emergence of biomarkers for individualized radiotherapy, several other characteristics, *e.g.*, cancer stem cell density, immune infiltrate, or tumor cell hypoxia [*e.g.* 35–37] should be thoroughly investigated. While current imaging techniques lack the sensitivity or spatial resolution to register ME, quantitative image features [*e.g.* 38] of the primary tumor could be valuable prognosticators for it. Some such features were indeed identified [10,12], while others failed to reach significance. This problem can mostly be overcome with larger cohorts, but it would also be desirable to try and alleviate it with pooled analyses of the existing data, since such efforts would oblige investigators to tackle the issues noted above in a harmonized fashion.

Multi-centric analyses might also serve to explain the few discrepant results reported, which diminish the confidence with which margin suggestions derived from these data can be adopted in clinical practice. At present a tentative agreement can only be seen among some studies investigating ME in NSCLC, especially when contrasting its two major histological types, but this agreement must not be overstated in light of the aforementioned geometric uncertainties. The contradictory results reported in sub-analyses of different histological grades of NSCLC hint at as yet poorly understood influences on ME, which require urgent clarification.

A more detailed understanding of the spatial distribution of clonogenic cells could aid treatment planning beyond the provision of adequate margin widths. Since cell density decreases towards the target edge, the dose delivered to these regions can also be reduced without relinquishing tumor control. This can, in turn, facilitate normal tissue sparing or central isotoxic dose escalation. A number of modeling studies have shown the feasibility of this [*e.g.* 39,40], but efforts are hampered by the lack of data on which to optimize dose distributions.

Existing data has been used to show that control of sub-clinical disease is partly accomplished by generous setup margins and the comparatively large volumes receiving low doses with current intensity-modulated techniques [*e.g.* 7,41,42]. The reduction in PTV margins afforded by image guidance and the steeper dose fall-off inherent to particle therapy might respectively limit these beneficial aspects.

The reported studies on recurrence patterns have consistently identified the GTV as the dominant site of failure, some suggesting the omission of a CTV expansion in favor of isotoxic dose escalation. By the argument above such proposals should be regarded with caution when transitioning to more advanced techniques, and recurrence patterns need to be continually monitored.

The difficulty in locating the origin of recurrence represents a major source of uncertainty. Coupled with the fact that all studies required complete radiographic response, it does, however, demonstrate that there is some distribution of sub-clinical disease during and after treatment. Only recently, a study on treatment failure after adaptive IMRT in advanced stage NSCLC patients has been published [43]. The particular adaptation strategy did not react to shrinkage of the GTV and the criterion for margin failures was rather broad, such that several questions are left open: *e.g.*, 1) whether the initial uniform CTV margin is still appropriate when treatment is adapted to reduced GTV size, 2) whether this holds true for different primary tumors, and 3) whether daily online patient setup is a pre-requisite for treatment adaptation. It is therefore crucial to treat patients undergoing adaptive protocols in the context of a prospective registration trial.

These remarks also, and in particular, hold true for particle beam irradiation. In order to thoroughly assess treatment outcome, therapy-related toxicity, and the reason for potential tumor recurrence, all patients undergoing proton or ion radio(chemo)therapy should be included in clinical studies which, among other assessments, produce thorough imaging-based follow-up.

After immense improvements in GTV definition and the derivation of institution-dependent PTV margins, the CTV is now the least well-understood piece of the target volume concept. This should give pause to those hastening to reduce CTV margins and serve as motivation to improve the way in which the CTV is defined and treated.

References

[1] Troost E, Thorwarth D, Oyen W. Imaging-based treatment adaptation in radiation oncology. J Nucl Med 2015;56:1922–9. http://dx.doi.org/10.2967/jnumed.115.162529.

[2] van Herk M, Remeijer P, Lebesque J. Inclusion of geometric uncertainties in treatment plan evaluation. Int J Radiat Oncol Biol Phys 2002;52:1407–22.

[3] Moghaddasi F, Bezak E, Marcu L. Current challenges in clinical target volume definition: tumour margins and microscopic extensions. Acta Oncol 2012;51:984–95. http://dx.doi.org/10.3109/0284186X.2012.720381.

[4] Kara M, Sak S, Orhan D, Yavuzer S. Changing patterns of lung cancer; (3/4 in.) 1.9 cm; still a safe length for bronchial resection margin? Lung Cancer 2000;30:161–8.

[5] Giraud P, Antoine M, Larrouy A, Milleron B, Callard P, De Rycke Y, et al. Evaluation of microscopic tumor extension in non-small-cell lung cancer for three-dimensional conformal radiotherapy planning. Int J Radiat Oncol Biol Phys 2000;48:1015–24. http://dx.doi.org/10.1016/S0360-3016(00)00750-1.

[6] Li W, Yu J, Liu G, Zhong W, Li W, Zhang B. A comparative study on radiology and pathology target volume in non-small-cell lung cancer. Zhonghua Zhong Liu Za Zhi 2003;25:566–8.

[7] Grills I, Fitch D, Goldstein N, Yan D, Chmielewski G, Welsh R, et al. Clinicopathologic analysis of microscopic extension in lung adenocarcinoma: defining clinical target volume for radiotherapy. Int J Radiat Oncol Biol Phys 2007;69:334–41. http://dx.doi.org/10.1016/j.ijrobp.2007.03.023.

[8] Weichert W, Warth A. Early lung cancer with lepidic pattern: adenocarcinoma in situ, minimally invasive adenocarcinoma, and lepidic predominant adenocarcinoma. Curr Opin Pulm Med 2014;20:309–16. http://dx.doi.org/10.1097/MCP.0000000000000065.

[9] Travis W, Brambilla E, Noguchi M, Nicholson A, Geisinger K, Yatabe Y, et al. International association for the study of lung cancer/american thoracic society/european respiratory society international multidisciplinary classification of lung adenocarcinoma. J Thorac Oncol 2011;6:244–85. http://dx.doi.org/10.1097/JTO.0b013e318206a221.

[10] Meng X, Sun X, Mu D, Xing L, Ma L, Zhang B, et al. Noninvasive evaluation of microscopic tumor extensions using standardized uptake value and metabolic tumor volume in non-small-cell lung cancer. Int J Radiat Oncol Biol Phys 2012;82:960–6. http://dx.doi.org/10.1016/j.ijrobp.2010.10.064.

[11] Yu J, Li X, Xing L, Mu D, Fu Z, Sun X, et al. Comparison of tumor volumes as determined by pathologic examination and FDG-PET/CT images of non-small-cell lung cancer: a pilot study. Int J Radiat Oncol Biol Phys 2009;75:1468–74. http://dx.doi.org/10.1016/j.ijrobp.2009.01.019.

[12] van Loon J, Siedschlag C, Stroom J, Blauwgeers H, van Suylen R, Knegjens J, et al. Microscopic disease extension in three dimensions for non-small-cell lung cancer: development of a prediction model using pathology-validated positron emission tomography and computed tomography features. Int J Radiat Oncol Biol Phys 2012;82:448–56. http://dx.doi.org/10.1016/j.ijrobp.2010.09.001.

[13] Stroom J, Blaauwgeers H, van Baardwijk A, Boersma L, Lebesque J, Theuws J, et al. Feasibility of pathology-correlated lung imaging for accurate target definition of lung tumors. Int J Radiat Oncol Biol Phys 2007;69:267–75. http://dx.doi.org/10.1016/j.ijrobp.2007.04.065.
[14] Siedschlag C, van Loon J, van Baardwijk A, Rossi M, van Pel R, Blaauwgeers J, et al. Analysis of the relative deformation of lung lobes before and after surgery in patients with NSCLC. Phys Med Biol 2009;54:5483–92. http://dx.doi.org/10.1088/0031-9155/54/18/009.
[15] Caldas-Magalhaes J, Kasperts N, Kooij N, van den Berg C, Terhaard C, Raaijmakers C, et al. Validation of imaging with pathology in laryngeal cancer: accuracy of the registration methodology. Int J Radiat Oncol Biol Phys 2012;82:e289–98. http://dx.doi.org/10.1016/j.ijrobp.2011.05.004.
[16] Hiroto I, Nomura Y, Sueyoshi K, Mitsuhashi S, Ichikawa A. Pathological studies relating to neoplasms of the hypopharynx and the cervical esophagus. Kurume Med J 1969;16:127–33.
[17] Ho C, Ng W, Lam K, Wei W, Yuen A. Submucosal tumor extension in hypopharyngeal cancer. Arch Otolaryngol Head Neck Surg 1997;123:959–65.
[18] Campbell S, Poon I, Markel D, Vena D, Higgins K, Enepekides D, et al. Evaluation of microscopic disease in oral tongue cancer using whole-mount histopathologic techniques: implications for the management of head-and-neck cancers. Int J Radiat Oncol Biol Phys 2012;82:574–81. http://dx.doi.org/10.1016/j.ijrobp.2010.09.038.
[19] Siu K, Cheung H, Wong J. Shrinkage of the esophagus after resection for carcinoma. Ann Surg 1986;203:173–6.
[20] Tsutsui S, Kuwano H, Watanabe M, Kitamura M, Sugimachi K. Resection margin for squamous cell carcinoma of the esophagus. Ann Surg 1995;222:193–202.
[21] Lam K, Ma L, Wong J. Measurement of extent of spread of oesophageal squamous carcinoma by serial sectioning. J Clin Pathol 1996;49:124–9.
[22] Gao X, Qiao X, Wu F, Cao L, Meng X, Dong Z, et al. Pathological analysis of clinical target volume margin for radiotherapy in patients with esophageal and gastroesophageal junction carcinoma. Int J Radiat Oncol Biol Phys 2007;67:389–96. http://dx.doi.org/10.1016/j.ijrobp.2006.09.015.
[23] Song Y, Liang Y, Zang R, Hu L, Zhu S. Application of serial section method to determine the radiotherapy target volume for esophageal squamous carcinoma. Cell Biochem Biophys 2013;66:351–6. http://dx.doi.org/10.1007/s12013-012-9473-8.
[24] Due A, Vogelius I, Aznar M, Bentzen S, Berthelsen A, Korreman S, et al. Methods for estimating the site of origin of locoregional recurrence in head and neck squamous cell carcinoma. Strahlenther Onkol 2012;188:671–6. http://dx.doi.org/10.1007/s00066-012-0127-y.
[25] Liang X, Yu H, Yu R, Xu G, Zhu G. Efficacy of the smaller target volume for stage III non-small cell lung cancer treated with intensity-modulated radiotherapy. Mol Clin Oncol 2015;3:1172–6. http://dx.doi.org/10.3892/mco.2015.588.
[26] Cai S, Shi A, Yu R, Zhu G. Feasibility of omitting clinical target volume for limited-disease small cell lung cancer treated with chemotherapy and intensity-modulated radiotherapy. Radiat Oncol 2014;9:17. http://dx.doi.org/10.1186/1748-717X-9-17.
[27] Kilburn J, Lucas J, Soike M, Ayala-Peacock D, Blackstock A, Hinson W, et al. Is a Clinical Target Volume (CTV) Necessary in the Treatment of Lung Cancer in the Modern Era Combining 4-D Imaging and Image-guided Radiotherapy (IGRT)? Cureus 2016;8:e466. http://dx.doi.org/10.7759/cureus.466.
[28] Dandekar V, Morgan T, Turian J, Fidler M, Showel J, Nielsen T, et al. Patterns-of-failure after helical tomotherapy-based chemoradiotherapy for head and neck cancer: implications for CTV margin, elective nodal dose and bilateral parotid sparing. Oral Oncol 2014;50:520–6. http://dx.doi.org/10.1016/j.oraloncology.2014.02.009.
[29] Due A, Vogelius I, Aznar M, Bentzen S, Berthelsen A, Korreman S, et al. Recurrences after intensity modulated radiotherapy for head and neck squamous cell carcinoma more likely to originate from regions with high baseline [18F]-FDG uptake. Radiother Oncol 2014;111:360–5. http://dx.doi.org/10.1016/j.radonc.2014.06.001.
[30] Vogelius I, Håkansson K, Due A, Aznar M, Berthelsen A, Kristensen C, et al. Failure-probability driven dose painting. Med Phys 2013;40:081717. http://dx.doi.org/10.1118/1.4816308.
[31] Bayman E, Prestwich R, Speight R, Aspin L, Garratt L, Wilson S, et al. Patterns of failure after intensity-modulated radiotherapy in head and neck squamous cell carcinoma using compartmental clinical target volume delineation. Clin Oncol 2014;26:636–42. http://dx.doi.org/10.1016/j.clon.2014.05.001.
[32] Oksuz D, Prestwich R, Carey B, Wilson S, Senocak M, Choudhury A, et al. Recurrence patterns of locally advanced head and neck squamous cell carcinoma after 3D conformal (chemo)-radiotherapy. Radiat Oncol 2011;6:54. http://dx.doi.org/10.1186/1748-717X-6-54.
[33] Ferreira B, Marques R, Khouri L, Santos T, Sá-Couto P. M. do Carmo Lopes, Assessment and topographic characterization of locoregional recurrences in head and neck tumours. Radiat Oncol 2015;10:41. http://dx.doi.org/10.1186/s13014-015-0345-4.
[34] De Felice F, Thomas C, Barrington S, Pathmanathan A, Lei M, Urbano T. Analysis of loco-regional failures in head and neck cancer after radical radiation therapy. Oral Oncol 2015;51:1051–5. http://dx.doi.org/10.1016/j.oraloncology.2015.08.004.
[35] Baumann M, Krause M, Overgaard J, Debus J, Bentzen S, Daartz J, et al. Radiation oncology in the era of precision medicine. Nat Rev Cancer 2016;16:234–49. http://dx.doi.org/10.1038/nrc.2016.18.
[36] Linge A, Löck S, Gudziol V, Nowak A, Lohaus F, von Neubeck C, et al. Low Cancer Stem Cell Marker Expression and Low Hypoxia Identify Good Prognosis Subgroups in HPV(-) HNSCC after Postoperative Radiochemotherapy: A Multicenter Study of the DKTK-ROG. Clin Cancer Res 2016;22:2639–49. http://dx.doi.org/10.1158/1078-0432.CCR-15-1990.
[37] Lohaus F, Linge A, Tinhofer I, Budach V, Gkika E, Stuschke M, et al. HPV16 DNA status is a strong prognosticator of loco-regional control after postoperative radiochemotherapy of locally advanced oropharyngeal carcinoma: results from a multicentre explorative study of the German Cancer Consortium Radiation Oncology Group (DKTK-ROG). Radiother Oncol 2014;113:317–23. http://dx.doi.org/10.1016/j.radonc.2014.11.011.
[38] Aerts H, Velazquez E, Leijenaar R, Parmar C, Grossmann P, Carvalho S, et al. Decoding tumour phenotype by noninvasive imaging using a quantitative radiomics approach. Nat Commun 2014;5:4006. http://dx.doi.org/10.1038/ncomms5006.
[39] South C, Partridge M, Evans P. A theoretical framework for prescribing radiotherapy dose distributions using patient-specific biological information. Med Phys 2008;35:4599–611. http://dx.doi.org/10.1118/1.2975229.
[40] Unkelbach J, Menze B, Konukoglu E, Dittmann F, Ayache N, Shih H. Radiotherapy planning for glioblastoma based on a tumor growth model: implications for spatial dose redistribution. Phys Med Biol 2014;59:771–89. http://dx.doi.org/10.1088/0031-9155/59/3/771.
[41] Siedschlag C, Boersma L, van Loon J, Rossi M, van Baardwijk A, Gilhuijs K, et al. The impact of microscopic disease on the tumor control probability in non-small-cell lung cancer. Radiother Oncol 2011;100:344–50. http://dx.doi.org/10.1016/j.radonc.2011.08.046.
[42] Selvaraj J, Baker C, Nahum A. Impact of microscopic disease extension, extra-CTV tumour islets, incidental dose and dose conformity on tumour control probability. Australas Phys Eng Sci Med 2016;39:493–500. http://dx.doi.org/10.1007/s13246-016-0446-x.
[43] Tvilum M, Khalil A, Møller D, Hoffmann L, Knap M. Clinical outcome of image-guided adaptive radiotherapy in the treatment of lung cancer patients. Acta Oncol 2015;54:1430–7. http://dx.doi.org/10.3109/0284186X.2015.1062544.